Thermal Conductivity of CaF_2, MnF_2, CoF_2, and ZnF_2 Crystals

GLEN A. SLACK
General Electric Research Laboratory, Schenectady, New York
(Received January 23, 1961)

The thermal conductivity of single crystals of CaF_2, MnF_2, CoF_2, and ZnF_2 has been measured over the temperature range from 3°K to 300°K. In this series, CaF_2 and ZnF_2 are diamagnetic, whereas MnF_2 and CoF_2 are antiferromagnetic. All four crystals have nearly equal thermal conductivities at room temperature, but differ at lower temperatures. CaF_2, which is nearly isotopically pure, exhibits an exponential rise in conductivity with decreasing temperature characteristic of umklapp processes. ZnF_2 shows only traces of such umklapp behavior because its conductivity is limited by isotope and impurity scattering. Small cusps are observed in the conductivities of MnF_2 and CoF_2 at their Néel temperatures of 67°K and 38°K, respectively, which indicate the presence of phonon-magnon scattering. Some experimental details concerning thermal conductivity measurements and the behavior of gold-cobalt thermocouples are also given.

INTRODUCTION

CRYSTALS of MnF_2 and CoF_2 exhibit a transition from paramagnetic behavior to antiferromagnetic behavior at their Néel temperatures,[1-4] T_N, of 67°K and 38°K, respectively. Anomalies in the thermal conductivity of antiferromagnetic crystals have been observed at T_N for MnO[5] and, in some recent experiments by the author, for CoO. The occurrence of such an anomaly is believed to be due to the rapid dying out of the phonon scattering caused by the magnetic system at temperatures below T_N. Therefore, anomalies in the thermal conductivity are to be expected in MnF_2 and CoF_2. Other types of anomalies in thermal conductivity versus temperature curves for insulators have been found, for example, in NH_4Cl[6] CH_4,[7] and $BaTiO_3$.[8] However, in these latter solids, an entirely different mechanism is responsible for the transitional behavior.

The purpose of the present study is to determine the effect of the magnetic behavior of MnF_2 and CoF_2 on the thermal conductivity. In order to have similar diamagnetic materials for comparison, crystals of CaF_2 and ZnF_2 were chosen. The problem here is to choose diamagnetic crystals which have nearly the same lattice dynamics as the antiferromagnetic crystals. Then the major differences will be in the magnetic properties.

COMPARISON OF CRYSTALS

The crystal structure of CaF_2 is cubic, and differs from the other three fluorides which all have the tetragonal SnO_2 structure. The CaF_2 crystal structure represents a simple cubic lattice of F^- ions only slightly enlarged by the introduction of the Ca^{++} ions. The MnF_2, CoF_2, and ZnF_2 represent what can be considered as a close-packed fcc lattice of F^{-1} ions somewhat distorted by the introduction of the smaller radius metal ions. Table I gives the ratio, r, of the metal ion radius to the fluorine ion radius, and the lattice constants,[9] a_0 and c_0 of all four fluorides. The larger r for CaF_2 compared to the other fluorides can be thought of as the cause of the shift from a fcc to a simple cubic packing of F^- ions. The simple cubic array of F^- ions has larger "interstitial" volumes. For comparison, the value of r in MgF_2 is 0.48, and the structure is again tetragonal.

The amount of distortion of the tetragonal crystals from true cubic can be visualized from the a_0/c_0 ratio. This ratio should be $\sqrt{2}$ for a cubic crystal. The values of $a_0/(c_0\sqrt{2})$ in Table I vary from 1.04–1.06. This means the distortion from cubic is slight for MnF_2, CoF_2, or ZnF_2, and that the amount of this distortion is comparable for all three. The thermal conductivity at 300°K and above is rather insensitive to details of the crystal structure. It depends[10,11] on such average parameters as M, V_0, and θ. Table I shows that all four crystals are quite similar in these respects.

The average sound velocities in Table I have been computed or estimated for a temperature of 0°K. For CaF_2 the elastic constant data of Huffman and Norwood[12] was used to compute the longitudinal and transverse sound velocities v_l and v_t. An average sound velocity of phonons, $\bar{v}_g$, was computed from these by weighting in favor of the transverse velocity using the following approximation:

$$\bar{v}_g = v_t \frac{2 + [v_t/v_l]^2}{2 + [v_t/v_l]^3}. \tag{1}$$

This weighting is equivalent to the one used by Casimir[13]

[1] M. Griffel and J. W. Stout, J. Chem. Phys. **18**, 1455 (1950).
[2] J. W. Stout and L. M. Matarrese, Revs. Modern Phys. **25**, 338 (1953).
[3] J. W. Stout and E. Catalano, J. Chem. Phys. **23**, 2013 (1955).
[4] D. F. Gibbons, Phys. Rev. **115**, 1194 (1959).
[5] G. A. Slack and R. Newman, Phys. Rev. Letters **1**, 359 (1958).
[6] C. V. Simson, Naturwissenschaften **38**, 559 (1951).
[7] A. N. Gerritsen and P. van der Star, Physica **9**, 503 (1942).
[8] I. Yoshida, S. Nomura, and S. Sawada, J. Phys. Soc. Japan **13**, 1550 (1958).

[9] J. W. Stout and S. A. Reed, J. Am. Chem. Soc. **76**, 5279 (1954).
[10] G. Leibfried and E. Schlömann, Nachr. Akad. Wiss. Göttingen, Math.-physik. Kl. 4, 71 (1954).
[11] P. G. Klemens, *Solid-State Physics*, edited by F. Seitz and D. Turnbull (Academic Press, Inc., New York, 1958), Vol. 7, pp. 1, 46.
[12] D. R. Huffman and M. H. Norwood, Phys. Rev. **117**, 709 (1960).
[13] H. B. G. Casimir, Physica **5**, 495 (1938).

TABLE I. Physical constants of some divalent fluoride crystals.[a]

Crystal	r	a_0 (Å)	c_0 (Å)	$a_0/c_0\sqrt{2}$	V_0 (Å³)	M (g)	ρ (g/cm³)	$\bar{v}_g$ (10⁵ cm/sec)	θ at 0°K	θ at 30°K	θ at 300°K	K_θ' (w/cm deg)	$\bar{K}_\theta$ (w/cm deg)
CaF₂	0.73	5.462	...	...	40.74	78.08	3.181	3.51	508	470	500	0.069	0.061
MnF₂	0.59	4.873	3.310	1.041	39.30	92.94	3.925	(3.0)	(450)	...	510	0.082	0.056
CoF₂	0.53	4.695	3.180	1.044	35.05	96.94	4.592	(2.9)	(450)	...	510	0.084	0.041
ZnF₂	0.54	4.703	3.134	1.061	34.66	103.38	4.952	(2.9)	(450)	380	510	0.090	0.054

[a] r =ratio of metal ion radius to fluorine ion radius, a_0 and c_0 =lattice constants, V_0 =molecular volume, M =molecular weight, ρ =x-ray crystal density, $\bar{v}_g$ =average sound velocity, θ =Debye temperature, K_θ' =value of thermal conductivity at $T=\theta$, calculated from Eq. (2), $\bar{K}_\theta$ =average experimental value of thermal conductivity at $T=\theta$ from Eq. (6), and ( ) =an estimated value.

in analyzing the boundary scattering of phonons. This is justifiable since one of the main uses of $\bar{v}_g$ will be in computing the boundary scattering limit. A straight 2 to 1 weighting of v_t in an arithmetic average would give an average velocity of 4.7×10^5 cm/sec for CaF₂ instead of 3.5×10^5 cm/sec. The $\bar{v}_g$ values for the other fluorides were estimated from the $\bar{v}_g$ of CaF₂ and from the θ (0°K) and V_0 values in Table I.

The Debye temperatures for CaF₂ and ZnF₂ have been calculated from heat capacity measurements.[3,12,14,15] In general, θ is a function of temperature, so Table I includes the high- and low-temperature θ limits at 300°K and at 0°K. The minimum value of θ occurs at about 30°K for CaF₂ and ZnF₂, and is given in Table I. The heat capacities of the MnF₂ and CoF₂ include a magnetic contribution, so that some subtraction scheme is necessary to obtain the lattice specific heat. The average lattice Debye temperatures have been taken from the estimates in the literature.[3,16] These averages come so close to the Debye temperature of ZnF₂ that this value has been taken for MnF₂ and CoF₂ as well. The θ (30°K) values for MnF₂ and CoF₂ are quite uncertain because of the nearness of T_N, and have not even been estimated.

Assuming that the only carriers of heat energy are phonons, then the thermal conductivity at a temperature equal to θ can be estimated from the theory.[10,11] This assumes that the only phonon scattering mechanism is other phonons. As Klemens[11] has shown, this theory gives values of the thermal conductivity, K_θ', at a temperature equal to θ which is too large by about a factor of 4 for the alkali halides. In the following expression, the value of K_θ' is set equal to just one-fourth that given by the theory[10]:

$$K_\theta' = 3.31\times10^6 (M\theta^2 V_0^{\frac{1}{3}}\gamma^{-2})\text{deg}^{-3}\text{ sec}^{-3}, \quad (2)$$

where M, θ, and V_0 are given in Table I. The M and V_0 are for the triatomic molecule. The Grüneisen constant,[17,18] γ, is 1.8 for CaF₂ at 300°K, and is taken to be

1.8 for the other three crystals for want of measured values. The K_θ' values in Table I computed from Eq. (2) are nearly the same for all four crystals, and are within a factor of 2 of the average values extrapolated to $T=\theta$ deduced from Fig. 11 and Eq. (6).

So far it has been shown that the four crystals are quite similar in their lattice properties, and that the thermal conductivities are nearly alike in the temperature range where phonon-phonon scattering is dominant. At lower temperatures other scattering mechanisms enter the picture. One basic difference is the isotopic constitution of the elements in the crystals. It has been shown that isotopes can be effective phonon scatterers at low temperatures.[19-21] The three elements Mn, Co, and F have a single naturally occurring isotope, so that there will be no isotope scattering in MnF₂ or CoF₂. The CaF₂ should have a small isotope scattering since Γ^{19} of natural[22] calcium is 2.46×10^{-5}. The value of Γ for isotopes is determined from

$$\Gamma = \frac{1}{12}\sum_j f_j\left(\frac{m_j-\bar{m}}{\bar{m}}\right)^2, \quad \bar{m}=\sum_j f_j m_j, \quad (3)$$

where f_j is the fractional concentration of an isotope of mass m_j. The value of Γ in Eq. (3) is the same as the Γ used in reference 23, but is the $B\Gamma$ of reference 19 with $B=1/12$. The theoretical value of $B=1/12$ is used now, instead of the empirical value of $\frac{1}{3}$ found in reference 19.

The Γ of CaF₂ is less than the Γ of Ca by the ratio

$$\Gamma(\text{CaF}_2)/\Gamma(\text{Ca}) = (\text{mass of Ca/mass of CaF}_2)^2, \quad (4)$$

which makes $\Gamma(\text{CaF}_2)=0.65\times10^{-5}$. For ZnF₂, the computed $\Gamma(\text{ZnF}_2)=1.98\times10^{-5}$, which is three times as large as that for CaF₂. So far only isotopes have been considered in computing Γ.

Both isotopes and chemical impurities can act as point scatterers of phonons. Hence chemical impurities of different mass or of different ionic charge than those of the host lattice can reduce the thermal conductivity

[14] A. Eucken and F. Schwers, Ber. deut. physik. Ges. 15, 578 (1913).
[15] S. S. Todd, J. Am. Chem. Soc. 71, 4115 (1949).
[16] J. A. Hofmann, A. Paskin, J. K. Tauer, and R. J. Weiss, J. Phys. Chem. Solids 1, 45 (1956).
[17] E. Grüneisen, Handbuch der Physik, edited by S. Flügge (Verlag Julius Springer, Berlin, Germany, 1926), Vol. 10, p. 1.
[18] R. Srinivasan, J. Indian Inst. Sci. 38A, 201 (1956).

[19] G. A. Slack, Phys. Rev. 105, 829 (1957).
[20] R. Berman, E. L. Foster, and J. M. Ziman, Proc. Roy. Soc. (London) A237, 344 (1956).
[21] T. H. Geballe and G. W. Hull, Phys. Rev. 110, 773 (1958).
[22] D. Strominger, J. M. Hollander, and G. T. Seaborg, Revs. Modern Phys. 30, 585 (1958).

TABLE II. Chemical impurity content of the crystals as determined by quantitative spectrographic analysis.

Crystal	Source	Al	Be	Ca	Fe	Li	Mg	Mn	Na	Ni	Pb	Sr
						Impurity concentration, $\log_{10}\epsilon_{pj}$ (e)						
CaF₂	a	18.1	18.3	⋯	<17.6	18.4	<17.6	<17.2	17.9	<18.0	<17.0	18.6
MnF₂	b	18.3	<18.4	17.7	18.1	<18.2	19.7	⋯	18.0	<17.7	<17.1	<17.4
CoF₂	c	18.8	<18.1	20.2	19.9	<18.3	20.2	19.4	18.1	20.4	19.2	<17.4
ZnF₂	d	18.1	18.4	17.9	19.1	18.4	<18.1	18.1	<18.8	19.2	<17.2	17.5

a Harshaw Chemical Company, Cleveland 6, Ohio.
b Courtesy of J. W. Nielsen and S. Foner.
c Grown by R. Newman at the General Electric Research Laboratory.
d Grown by P. D. Johnson at the General Electric Research Laboratory.
e The concentration ϵ_{pj} of chemical impurities of type j is given in terms of the number of impurity atoms per cm³. In order to simplify the table, $\log_{10}\epsilon_{pj}$ is given.

of a crystal.[21,23–26] Careful spectrographic analyses were made of the crystals used in this experiment. The results are shown in Table II.

A total of 31 different metallic elements were checked for in each crystal. In Table II are listed all of those elements present in quantities greater than 3×10^{18}/cm³. As an average there were 20 elements at concentrations known to be $<3\times10^{18}$/cm³; of these, 14 were known to be $<1\times10^{18}$/cm³; and 8 were known to be $<3\times10^{17}$/cm³. Many were below the limits of detectability. If all the known concentrations listed in Table II are added up without regard to the specific kind of impurity, the result for CaF₂, MnF₂, or ZnF₂ is a total impurity content of about 2×10^{19}/cm³. The impurity content of 8×10^{20}/cm³ in the CoF₂ is higher by 40 times. No better CoF₂ single crystals were available when the measurements were made.

The impurity content in the Harshaw CaF₂ is a factor of about 4 less than that reported for the powdered material by Ure.[27] As a check for the presence of CaO contamination in the CaF₂ crystal, the optical absorption[28] was measured in the ultraviolet between 5 and 10 ev. No absorption peaks were seen at 6 ev, and the absorption coefficient α here was less than 0.3 cm⁻¹. The absorption started rising rapidly at 10 ev. From the upper limit of α at 6 ev, the oxygen content is tentatively estimated to be less than 100 ppm.

At temperatures below about 10°K, the dislocations[29] and the crystal boundaries[13] become important as phonon scatterers. The theory of dislocation scattering is not reliable as to order of magnitude, but an estimate of the effect can be obtained from experiment.[29] If ZnF₂ behaves anything like LiF does, then it would take about 5×10^7 dislocations to account for the low thermal conductivity below 10°K. The dislocation density in the present crystals was not measured, but probably varies between 10^4 and 10^5 cm⁻², since they were carefully cut

and handled after growth from the melt. Thus we shall take no further account of this scattering mechanism.

The crystal size, however, is important in determining the boundary scattering, and is given in Table III. The rod shaded samples of length S all had a rectangular cross section of area A. The effective diameter d of the rod was computed from $d=(4A/\pi)^{\frac{1}{2}}$. Since the thermal conductivity in a tetragonal crystal is anisotropic, it is also necessary to know the crystal orientation. The angle between the tetragonal c axis and the direction of heat flow is also given in Table III.

EXPERIMENTAL DETAILS

The thermal conductivity of the samples was measured in the apparatus shown in Fig. 1. Similar apparatuses have been mentioned before.[23,25,26,29] In order to cover the temperature range from 3–300°K, use was made of He, H₂, N₂, C₂H₅OH+solid CO₂, and H₂O as cryogenic liquids. This arrangement allowed the measurement of thermal conductivity under steady state conditions over the whole temperature range. Heat was supplied to the crystal by a 1000-ohm nichrome wire heater at the top of the crystal. The power input was determined to ±1% by ammeter and voltmeter measurements, and varied from 2×10^{-4} w to 1 w depending on the temperature and the sample. The heat then flowed out to the center plate of the apparatus and through the copper variable thermal resistors to the bath. The crystal samples inside the inner can were were measured in a vacuum of about 10^{-6} mm Hg, which was continuously pumped. An outer can was

TABLE III. Shape and orientation of the fluoride crystals.[a]

Crystal	Run No.	Orientation	S (cm)	d (cm)
CaF₂	30	⋯	4.8	0.88
MnF₂	18	90°	1.1	0.13
MnF₂	19	90°	0.93	0.26
MnF₂	20	0°	0.99	0.25
CoF₂	44	?	0.40	0.16
CoF₂	45	26°	0.45	0.13
ZnF₂	40	74°	1.2	0.24

a Run No. refers to the experimental run in which the thermal conductivity was measured. The orientation is the angle between the direction of heat flow and the c axis. S =length of the sample. d =effective diameter of the sample from $d = (4A/\pi)^{\frac{1}{2}}$.

23 G. A. Slack, Phys. Rev. 105, 832 (1957).
24 R. Berman, P. T. Nettley, F. W. Sheard, A. N. Spencer, R. W. H. Stevenson, and J. M. Ziman, Proc. Roy. Soc. (London) A253, 403 (1959).
25 R. O. Pohl, Phys. Rev. 118, 1499 (1960).
26 W. S. Williams, Phys. Rev. 119, 1021 (1960).
27 R. W. Ure, J. Chem. Phys. 26, 1363 (1957).
28 A. Smakula, Z. Physik 138, 276 (1954).
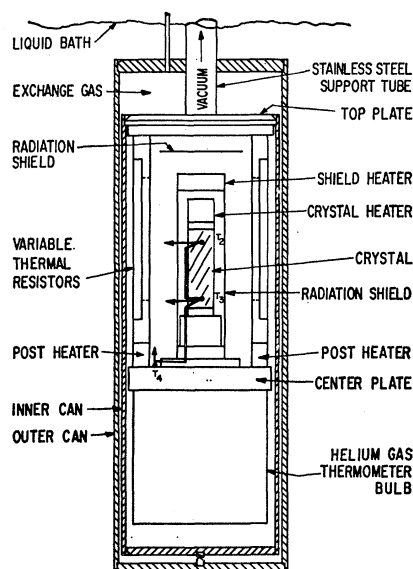29 R. L. Sproull, M. Moss, and H. Weinstock, J. Appl. Phys. 30, 334 (1959).

FIG. 1. A schematic of the experimental chamber showing the crystal, the thermocouples, the heater, and associated equipment. This chamber is totally immersed in the cryogenic liquid.

occasionally used to surround the inner can with a variable pressure exchange gas of He between the two. This scheme usually proved to be unnecessary since liquid H_2 was readily available. If no liquid H_2 is available, it offers a convenient method of varying the thermal resistance between the sample and the bath during the course of an experimental run. With liquid H_2 available, sufficient control over the average sample temperature was provided by the combination of crystal and post heaters.

The apparatus is also supplied with a radiation shield around the sample so that the effects of thermal radiation above 200°K can be eliminated. This was not used for the present samples since their thermal conductivities above 200°K are relatively high. For example, had it been used, the 302°K point in Fig. 5 probably would have been about 20% lower.

The thermal contacts to the crystal samples varied with the specimen. For the CaF_2 spring-loaded, indium-faced clamps made of OFHC copper were used.[29] For the other samples, which were considerably smaller, Ni or Mo contact plates were cemented to the sample with either a thermosetting epoxy resin, Araldite AN-100,[30] or a room temperature curing activated epoxy resin filled with Al_2O_3 powder, Armstrong A-2.[31] The thickness of the cement layer has to be kept small ($\leq 25\ \mu$) since the thermal conductivity of these cements is low. For the A-2, approximate values of thermal conductivity are 4×10^{-3} watt/cm deg at 300°K and 10^{-5} watt/cm deg at 4°K. The Ni or Mo contact plates were then attached to the center plate of the apparatus with screws. A 0.01-cm thick sheet of indium foil was used to

insure good thermal contact between the contact and center plates.

Thermocouples

The temperatures along the sample were measured with 0.0075-cm diameter differential thermocouples made from gold-cobalt[32] (98.2% Au, 1.8% Co) versus manganin[33] (83% Cu, 13% Mn, 4% Ni, 0.3% Fe). All alloy compositions given here are in atomic percent. The scheme is shown in Fig. 1 where a chain of three thermocouple junctions measures the temperature differences $(T_2 - T_3)$ and $(T_3 - T_4)$. The temperature T_4 is measured to ± 0.05°K by means of a constant volume helium gas thermometer. The bulb volume of the gas thermometer is 86 cm^3, and is connected to a manometer at room temperature via a 0.11-cm i.d. capillary. The output of these differential thermocouples was measured with a potentiometer above 30°K, or a modified dc breaker amplifier[34] at lower temperatures. At an amplifier gain of 10^7, thermocouple voltages of 10^{-7} v can be measured to $\pm 5\%$ with a time constant of 1 sec. At higher voltages, the accuracy is $\pm 2\%$. With this arrangement, values of $2(T_2 - T_3)/(T_2 + T_3)$ from 0.05%–15% were measured, an average value being about 2%.

The absolute thermoelectric power $S(T)$ at temperature T of the gold-cobalt and of the manganin wires was determined using the absolute thermoelectric power scale of Christian et al.[35] for Pb as a basis. This Pb scale was applied to the earlier results of Borelius et al.[36] on silver-normal (99.63% Ag+0.37% Au) in order to yield the absolute thermoelectric power of silver-normal versus temperature. This revised silver-normal scale differs slightly from that of Borelius et al.[37] below 20°K, and is a constant 0.03 μv/deg less than theirs above 20°K. The gold-cobalt, manganin, and Chromel-P[38] (89% Ni, 11% Cr) were measured against silver-normal, and the $S(T)$ curves are shown in Fig. 2. The gold-cobalt has large and negative S values, while silver-normal and manganin have small positive values. The Chromel-P has moderately large positive values of S. The values of S below 10°K for silver-normal, manganin, and Chromel-P are only approximate, since such small values are difficult to measure.

In using thermocouples for thermal conductivity measurements, the thermal conductivity of the thermocouple wire itself should be small, especially at low temperatures. Values of the absolute thermoelectric power $S(T)$ and of the thermal conductivity $K(T)$ for

[30] CIBA Products Corporation, Fair Lawn, New Jersey.
[31] Armstrong Products Company, Warsaw, Indiana.
[32] Sigmund Cohn Corporation, Mount Vernon, New York.
[33] Driver-Harris Company, Harrison, New Jersey.
[34] M. D. Liston, C. E. Quinn, W. E. Sargeant and G. G. Scott, Rev. Sci. Instr. 17, 194 (1946).
[35] J. W. Christian, J. P. Jan, W. B. Pearson, and I. M. Templeton, Proc. Roy. Soc. (London) A245, 213 (1958).
[36] G. Borelius, W. H. Keesom, C. H. Johansson, and J. O. Linde, Proc. Acad. Sci.-Amsterdam 34, 1365 (1931).
[37] G. Borelius, W. H. Keesom, C. H. Johansson, and J. O. Linde, Proc. Acad. Sci.-Amsterdam 35, 10 (1932).
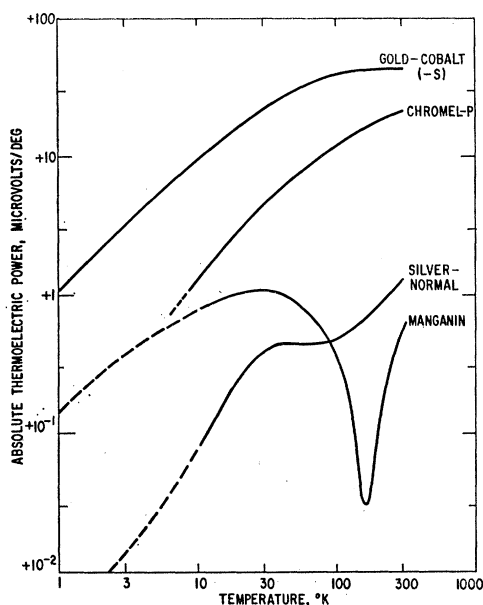[38] Hoskins Manufacturing Company, Detroit, Michigan.

FIG. 2. The absolute thermoelectric power S as a function of temperature for four different thermocouple wires. The S values are positive for all except gold-cobalt, which has a negative absolute thermoelectric power.

$T=10$ and 273.2°K are given in Table IV for gold-cobalt, manganin, and for other materials which have been used with gold-cobalt. Silver-normal has been used by Borelius et al.[39] and by Keesom and Matthijs[40]; copper has been used by Fuschillo,[41] by Powell and Bunch,[42] and by Greig[43]; constantan by Sproull et al.,[29] Pohl,[25] and Williams[26]; Chromel-P has been used by Corbett.[44] In Table IV, the absolute thermoelectric force at 273.2°K, $E(273.2)$ is also given for purposes of comparison. The value of $E(T)$ is defined by

$$E(T)=+\int_0^T S(T')dT'. \qquad (5)$$

From Table IV, it can be seen that only manganin and Chromel-P have thermal conductivities low enough to match that of gold-cobalt plus adequate thermoelectric properties compared to gold-cobalt over the temperature range from 3°K–300°K. Thus, thermocouples of manganin versus gold-cobalt or Chromel-P versus gold-cobalt would be useful. Manganin was used in the present experiment. The Chromel-P would have had the advantage of a large positive $S(T)$, which varies smoothly with temperature. The $S(T)$ of magnanin is

small, however, so the peculiar temperature variation, typical of copper-manganese alloys,[45] is not a serious drawback.

TABLE IV. Thermoelectric and thermal conductivity values for various thermocouple materials. $E(T)$ = absolute thermoelectric force at temperature T. $S(T)$ = absolute thermoelectric power at temperature T. $K(T)$ = thermal conductivity at temperature T. All alloy percentages are given in atomic %.

Material	$E(273.2)$ (μv)	$S(10)$ (μv/deg)	$S(273.2)$ (μv/deg)	$K(10)$ (watt/cm deg)	$K(273.2)$ (watt/cm deg)
Gold-cobalt[a]	−9910	−9.5	−43.0	0.04[h]	∼0.5[h]
Constantan[b]	−5850	−2.9	−36.0	0.04[k]	0.23[k]
Manganin[c]	+110	+0.8	+0.4	0.04[l]	0.21[k]
Silver-normal[d]	+180	+0.1	+1.2	∼2.0[l]	3.8[k]
Copper[e]	+350	0.0[g]	+1.9	8.7[m]	4.0[m]
Chromel-P[f]	+3020	+1.2	+21.0	∼0.04[l]	∼0.2[l]

[a] 98.2% Au, 1.8% Co; from reference 32.
[b] 52% Cu, 46% Ni, 2% Mn, Cupron; Wilbur B. Driver, Newark, New Jersey.
[c] 83% Cu, 13% Mn, 4% Ni, 0.3% Fe; from reference 33.
[d] 99.63% Ag, 0.37% Au; from reference 32.
[e] Electrolytic tough pitch copper.
[f] 89% Ni, 11% Cr; from reference 38.
[g] Reference 46.
[h] Reference 47.
[k] R. L. Powell and W. A. Blanpied, U. S. Natl. Bur. Standards Cir. No. 556 (1954).
[l] Estimated from reference k and electrical resistivity.
[m] Reference 48.

The thermoelectric behavior of gold-cobalt alloys depends upon the cobalt concentration, as has been shown before.[39,40] Since this alloy has seen rather wide use, it is worthwhile to consider how the S and E values depend on the cobalt concentration. Since $E(273.2)$ is the integral of $S(T)$ weighted for the large S values at high temperature, the value of S at some low temperature, like $S(10)$, combined with $E(273.2)$ will give a representative picture of this dependence for the whole temperature range. Approximate values of these functions versus the concentration of cobalt are given in Fig. 3. The main problem in constructing Fig. 3 was to determine the cobalt concentration accurately.

The electrical resistivity at 273.2°K of Au-Co alloys has been measured by Linde[49,50] and by Thomas.[51] Using Linde's data, the atomic percent of Co was computed for the present samples, and also for the same spool of wire as used by Fuschillo.[41] Note that these results on a nominal composition of 2.11% Co give actual concentrations of cobalt in solid solution from 1.2–2.0% on wire from Sigmund Cohn.[32] Other data points in Fig. 3 are taken from the work of Borelius et al.,[39] Keesom and Matthijs,[40] and Youngblood,[52] using their stated values of the cobalt concentration. From

[39] G. Borelius, W. H. Keesom, C. H. Johansson, and J. O. Linde, Proc. Acad. Sci.-Amsterdam 35, 15 (1932).
[40] W. H. Keesom and C. J. Matthijs, Physica 2, 623 (1935).
[41] N. Fuschillo, J. Phys. Chem. 61, 644 (1957).
[42] R. L. Powell and M. D. Bunch, Problems of Low-Temperature Physics and Thermodynamics (Pergamon Press, New York, 1959), p. 129.
[43] D. Greig, Phys. Rev. 120, 358 (1960).
[44] J. Corbett, private communication.

[45] F. A. Otter, J. Appl. Phys. 27, 197 (1956).
[46] A. V. Gold, D. K. C. MacDonald, W. B. Pearson, and I. M. Templeton, Phil. Mag. 5, 765 (1960).
[47] R. L. Powell, M. D. Bunch, and E. F. Gibson, J. Appl. Phys. 31, 504 (1960).
[48] R. L. Powell, W. M. Rogers, and H. M. Roder, J. Appl. Phys. 28, 1282 (1957).
[49] J. O. Linde, Ann. Physik 10, 52 (1931).
[50] A. N. Gerritsen, Physica 25, 489 (1959).
[51] J. L. Thomas, J. Research Natl. Bur. Standards 14, 589 (1935).
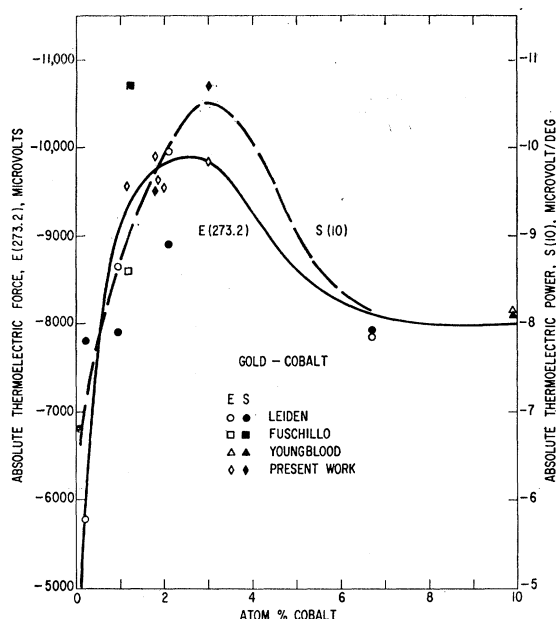[52] J. Youngblood, private communication.

FIG. 3. The absolute thermoelectric force at 273.2°K, $E(273.2)$, and the absolute thermoelectric power at 10°K, $S(10)$, for gold-cobalt alloys as a function of the cobalt concentration. The data are taken from various sources as noted.

Fig. 3, it is apparent that different calibration curves can be obtained from different batches of wire.

The Au-Co phase diagram has been carefully studied,[53] and Co in Au exhibits retrograde solubility. The extrapolated equilibrium solubility of cobalt in gold at room temperature is about 10^{-6} at.%. This is in contrast to Borelius et al,[54] who assumed that the 2.1% Co alloy was not supersaturated. Thus, the cobalt in solution may slowly precipitate at room temperature, and change the calibration curve. As can be seen from Fig. 3, the amount of change in the calibration will depend on the initial cobalt concentration. The author has observed a decrease in $E(273.2)$ for a 1.8% Co alloy at a rate of about 0.6% per year over a period of several years at room temperature. A second batch of wire from Sigmund Cohn of 1.8% Co exhibited a decrease of <0.02% per year. Powell and Bunch[42] reported a decrease of about 1% per year for a similar alloy. This precipitation rate can be drastically increased by heating the wire to soldering temperatures of 200°C. Therefore, any calibration curves for Au-Co thermocouples should be used with caution. For example, Fuschillo's wire probably had been heat treated prior to calibration, since the electrical resistivity indicates a Co concentration of 1.2%.

It is, of course, dangerous to draw many conclusions from a graph of collected values such as Fig. 3. The existence of a peak of S or E versus concentration at

about 3% Co seems to be clear. This peak is similar to those found[39] for Au-Fe alloys at low Fe concentrations. A peak was not well defined in the earlier work[39,40] on Au-Co alloys measured at widely spaced cobalt concentrations. It would appear that an alloy with 6–8% Co might be much more stable with respect to small changes in cobalt concentration than the normally used 2.1% Co alloy.

The gold-cobalt wire used in the present thermal conductivity experiments and listed in Table IV had a nominal composition of 2.11% Co. A chemical analysis of this particular batch of wire gave a total cobalt concentration of 1.98±0.03%. A measurement of the x-ray lattice parameter indicated[53] a solid solution cobalt concentration of 2.0±0.5%. The electrical resistivity measurements at 273.2°K gave 11.7×10^{-6} ohm-cm in
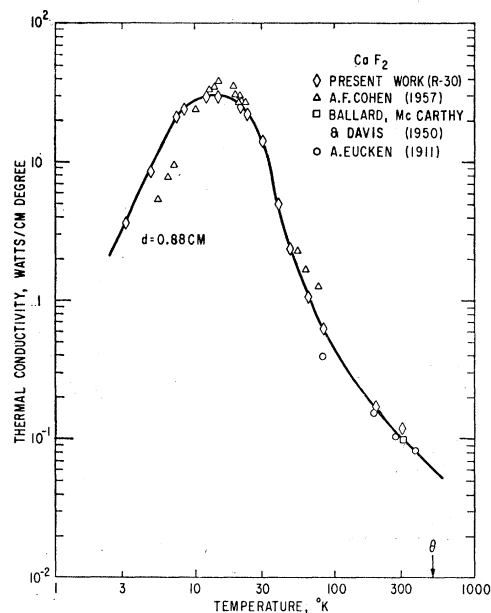

FIG. 4. A composite curve of the thermal conductivity of CaF_2 from 3°K–500°K. The Debye temperature is θ; the sample diameter d is 0.88 cm for Run-30.

the as received state, and 11.9×10^{-6} ohm-cm in an annealed state for an indicated 1.80% Co. Of all of these tests, it is felt that the electrical resistivity gives the best figure for the cobalt in solid solution. Thus a 1.8% Co concentration is taken for the thermocouple wire in Fig. 2.

EXPERIMENTAL RESULTS

Calcium Fluoride

The results of the present experiment on CaF_2 plus some of those of earlier studies are shown in Figs. 4 and 5. Fig. 4 shows the behavior in the low temperature region, and includes the data of Eucken,[55] Ballard,

[53] E. Raub and P. Walter, Z. Metallkunde 41, 234 (1950).
[54] G. Borelius, W. H. Keesom, C. H. Johansson, and J. O. Linde, Proc. Acad. Sci.-Amsterdam 35, 25 (1932).

[55] A. Eucken, Ann. Physik 34, 185 (1911).

McCarthy, and Davis,[56] and Cohen.[57,58] Although Cohen's work has been reported previously,[57,58] the author is indebted to A. F. Cohen for permission to quote her reported results here. Her crystal was also a Harshaw Chemical Company sample of chemical purity comparable to the present crystal (see Table II), and had an effective diameter of 0.31 cm. In Fig. 5, the collected data for CaF_2 from 200–400°K are given. This figure includes the work of the authors mentioned above[55–58] plus the data of Müller,[59] Charvat and Kingery,[60] Smoke and Koenig,[61] and McCarthy and Ballard.[62]

The present results obtained in experimental run number 30, i.e., R-30, are in satisfactory agreement with those of Cohen below 100°K. The smaller diameter of her sample accounts for most of the difference between Cohen's results and the present ones at temperatures below 10°K. The thermal conductivity found in R-30 at 300°K is, from Fig. 5, too large by 25%. This
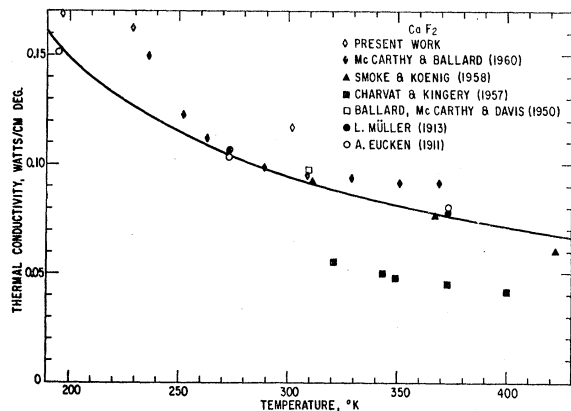

FIG. 5. A composite curve of the thermal conductivity of CaF_2 from 200°K–420°K. The present results lie somewhat above the curve because of uncorrected thermal radiation losses from the crystal and heater.

discrepancy is due to the fact that no correction or compensation for thermal radiation losses was made at 300°K. This radiation error is negligible at 100°K and below. The data of Charvat and Kingery appear to give values which are much lower than the present ones, and lower than the best-fit curve in Fig. 5 by about 40%. These data are therefore considered suspect.

[56] S. S. Ballard, K. A. McCarthy, and W. C. Davis, Rev. Sci. Instr. 21, 905 (1950).

[57] A. F. Cohen and L. C. Templeton, Bull. Am. Phys. Soc. 2, 188 (1957).

[58] A. F. Cohen, Proceedings of the Fifth International Conference on Low-Temperature Physics and Chemistry, Madison, Wisconsin, 1957 (University of Wisconsin Press, Madison, Wisconsin, 1958), p. 385.

[59] L. Müller, Phil. Diss. University Jena (1913), see reference 91.

[60] F. R. Charvat and W. D. Kingery, J. Am. Ceram. Soc. 40, 306 (1957).

[61] E. J. Smoke and J. H. Koenig; Rutgers, College of Engineering, Research Bull. No. 40 (1958).

[62] K. A. McCarthy and S. S. Ballard, J. Appl. Phys. 31, 1410 (1960).

The best-fit curve in Fig. 5 starts to rise more rapidly than T^{-1} with decreasing temperature for temperatures below $T/\theta = 0.5$. Below $T/\theta = 0.2$, the thermal conductivity rises exponentially with decreasing temperature to a maximum value of 30 watts/cm deg at 14°K.

Zinc Fluoride

In order to have a second diamagnetic crystal, ZnF_2 was chosen. In addition to this, the only other available data on a divalent fluoride are some on BaF_2.[62,63] Only one crystal of ZnF_2 was measured, and the results are shown in the composite Fig. 11. Its thermal conductivity is similar to that of CaF_2. Since its chemical and isotopic purity is rather low, the thermal conductivity shows only traces of the pronounced exponential rise that was found in CaF_2.

Manganese Fluoride

Three crystals of MnF_2 were measured in the present experiment, as indicated in Table III. The two samples with the 90° orientation (a axis) gave overlapping results. These together with those for the 0° orientation (c axis) are shown in Fig. 6. Notice that the thermal conductivity is anisotropic, with the thermal conductivity along the c axis K_c being larger than that along the a axis K_a. The ratio K_c/K_a approaches unity as the temperature decreases below 100°K.

Even though MnF_2 is isotopically pure, there is no pronounced exponential increase of conductivity with decreasing temperature, as was seen in CaF_2. However, there is a slight kink in the curve at the Néel temperature T_N of 67°K. The derivative $d \ln K_a(T)/d \ln T$
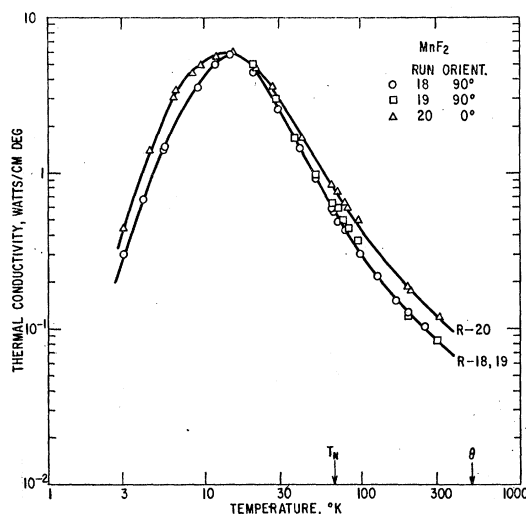

FIG. 6. The thermal conductivity of MnF_2 from 3°K–300°K. The thermal conductivity is anisotropic and has been measured with the heat flow at 0° and at 90° to the c axis. The Debye temperature is θ, and the Néel temperature is T_N.

[63] S. S. Ballard and K. A. McCarthy, J. Opt. Soc. Am. 41, 1062 (1951).

changes from -1.8 for temperatures just below T_N, to -1.6 for those just above T_N. The change for K_c is similar but somewhat smaller. This small change is not noticeable in the small scale graph of Fig. 6.

Cobalt Fluoride

The results for the two crystals of CoF_2 are shown in Fig. 7. These two crystals were of comparable chemical purity, but crystal R-44 had several cracks and flaws in it, whereas R-45 was a sound single crystal. This difference probably accounts for the lower conductivity of R-44. The conductivity of these crystals is in general lower than that of any of the others. This low conductivity is probably caused by the low purity. Notice, however, the pronounced minimum in the conductivity at the Néel temperature of 38°K. The points at 300°K are higher than the true thermal conductivity due to thermal radiation errors since no radiation shield was used. These have been omitted in drawing the curves in Fig. 7.

ANALYSIS OF THE RESULTS

Diamagnetic Crystals

In the diamagnetic, non-electrically-conducting crystals, CaF_2 and ZnF_2, all of the heat is transported by phonons. These are scattered by a combination of other phonons, chemical impurities, isotopes, and crystal boundaries. The dominant scattering mechanisms will be determined by the temperature and the concentration of scattering centers. At and somewhat below 300°K, the dominant scattering mechanism in both CaF_2 and ZnF_2 is other phonons. On this basis, we can compare the observed value of K at a temperature equal to the Debye temperature, $\bar{K}_\theta$, with the K_θ' value computed from Eq. (2) (see Table I). For the tetragonal
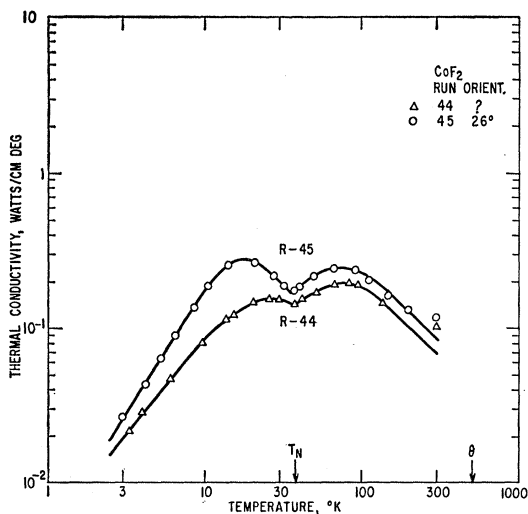

FIG. 7. The thermal conductivity of CoF_2 from 3°K–300°K. There is a minimum in the curve near the Néel temperature T_N, which is much lower than the Debye temperature, θ.

MnF_2, CoF_2, and ZnF_2, the average conductivity at $T=\theta$ is computed from

$$\bar{K}_\theta = \tfrac{2}{3}K_a + \tfrac{1}{3}K_c. \qquad (6)$$

Here K_a is the thermal conductivity measured when the heat flow is directed along the a axis, i.e., the crystal orientation is 90° in Table III. K_c refers to an orientation of 0°. $\bar{K}_\theta$ is given in Table I. For CoF_2 and ZnF_2, the anisotropy ratio K_c/K_a at $T=\theta$ was assumed to be the same as for MnF_2. This is reasonable since the ratio $a_0/(c_0\sqrt{2})$ is nearly the same for all three crystals (see Table I). The value of $\bar{K}_\theta$ for the CoF_2 and ZnF_2 were computed from the thermal resistivity ellipsoid method given by Nye[64] using $K_c/K_a = 1.42$.

If phonon-phonon scattering were the only source of thermal resistance in the crystal, then according to Peierls,[65] the thermal conductivity should rise exponentially with decreasing temperature. Leibfried and Schlömann[10] have suggested that the ratio $K(T)/K(\theta)$ should be a "universal" function of the reduced temperature, T/θ:

$$K(T)/K(\theta) = f(T/\theta). \qquad (7)$$

The exact function $f(T/\theta)$ was not specified.[10] This idea of a "universal" function is similar in approach to Keyes' analysis[66] of the behavior of the solidified gases. In crystals which are chemically and isotopically clean, the behavior of the observed ratio $K(T)/K(\theta)$ should be $f(T/\theta)$. The difficulty is to find such crystals. It has been shown[19] that solid He^4 [67] and Al_2O_3 [60,68,69] are sufficiently clean to exhibit the true exponential rise. Since then measurements on isotopically clean solid H_2,[70] solid He^3,[71] NaF,[72–74] CsI,[73,75] and Bi [76] have been made. There is sufficient data on all of these except CsI for some useful comparison. Consider a reduced thermal conductivity,

$$R(\tau) = \tau K(T)/K(\theta) = \tau f(\tau), \qquad (8)$$

where τ is a reduced temperature, $\tau = T/\theta$. In the temperature region $\tau \geq 1$, the value of R is unity since $K(T)$ varies as T^{-1}. If $K(T)$ rises more rapidly than T^{-1} as the temperature decreases below $\tau = 1$, then R will become greater than unity. A plot of $R(\tau)$ for a number

[64] J. F. Nye, *Physical Properties of Crystals* (Clarendon Press, Oxford, England, 1957), p. 199.

[65] R. Peierls, Ann. Physik **3**, 1055 (1929).

[66] R. W. Keyes, J. Chem. Phys. **31**, 452 (1959).

[67a] F. J. Webb, K. R. Wilkinson, and J. Wilks, Proc. Roy. Soc. (London) **A214**, 546 (1952). [b] F. J. Webb and J. Wilks, Phil. Mag. **44**, 664 (1953).

[68] R. Berman, E. L. Foster, and J. M. Ziman, Proc. Roy. Soc. (London) **A231**, 130 (1952).

[69] R. Berman, Proc. Phys. Soc. (London) **A65**, 1029 (1952).

[70] R. W. Hill and B. Schneidmesser, Z. physik. Chem. **16**, 257 (1958).

[71] E. J. Walker and H. A. Fairbanks, Phys. Rev. Letters **5**, 139 (1960).

[72] A. F. Cohen, J. Appl. Phys. **29**, 870 (1958).

[73] R. Berman, Z. physik. Chem. **16**, 145 (1958).

[74] A. Eucken and G. Kuhn, Z. physik Chem. **134**, 193 (1928).

[75] A. F. Cohen, Physica 24, S177 (1958).

[76] G. K. White and S. B. Woods, Phil. Mag. **3**, 342 (1958).

of isotopically pure solids and for CaF_2 is shown in Fig. 8. Note that for all of these solids some type of exponential rise is observed. The θ and K_θ values used in plotting the curves are given in Table V. For He^3, He^4, H_2, and Al_2O_3 the curves overlap, and it is assumed that these experimental results approximate a universal $R(\tau)$ function. The results for CaF_2 show a similar though somewhat smaller R function. The failure of CaF_2 to quite match the other results is probably caused by the small amounts of other isotopes in the Ca^{40}, and by the residual chemical impurities.

The $R(\tau)$ curves for Bi and NaF fall much below the others. It almost appears as though they have an effective Debye temperature which is much less than the one determined from specific heat measurements. Furthermore the calculated K_θ' value does not agree very well with the experimental K_θ value for Bi and NaF. The suggestion of a low effective Debye temperature

TABLE V. Density, Debye temperature, and thermal conductivity values for some nearly isotopically pure crystals. K_θ' = thermal conductivity at $T=\theta$ calculated from Eq. (2). K_θ = thermal conductivity at $T=\theta$ found experimentally.

Crystal	ρ (g/cm³)	θ (°K)	γ	K_θ' (watt/cm deg)	K_θ (watt/cm deg)
He⁴	0.208	29.3[a]	2?	2.7×10⁻⁵	
He³(β)	0.162	35?	2?	4.1×10⁻⁵	
H₂	0.088	100[b]	2?	2.4×10⁻⁴	
Bi	9.80	120[c]	2?	3.5×10⁻²	10.6×10⁻²
NaF	2.81	470[d]	2?	3.8×10⁻²	12.0×10⁻²
CaF₂	3.18	500[e]	1.8	6.9×10⁻²	6.1×10⁻²
Al₂O₃	3.98	1010[f]	3.0[g]	6.8×10⁻²	7.5×10⁻²

[a] J. S. Dugdale and F. E. Simon, Proc. Roy. Soc. (London) A218, 291 (1953); also reference 67.
[b] R. W. Hill and O. V. Lounasmaa, Phil. Mag. 4, 785 (1959).
[c] N. E. Phillips, Phys. Rev. 118, 644 (1960).
[d] S. S. Mitra and S. K. Joshi, Physica 26, 284 (1960).
[e] See Table I.
[g] G. T. Furukawa, T. B. Douglas, R. E. McCoskey and D. G. Ginnings J. Research Natl. Bur Standards 57, 67 (1956).
[g] Reference 11.

has been made by Geballe and Hull[21] to account for the lack of an exponential rise in isotopically enriched Ge. Such an argument shows that $f(\tau)$ is not really a universal function for all crystal lattices, but depends on the details of the phonon spectrum. However, in view of the lack of a good theoretical calculation of $f(\tau)$, it is useful to construct an approximate function from the results.

It has been shown by Peierls[65] that at low temperatures the thermal conductivity should increase exponentially with decreasing temperature as

$$K(\tau) = A\tau^\eta \exp(b^{-1}\tau^{-1}), \qquad (9)$$

where η and b are constants of the order of unity. For the present purposes η will be set equal to zero, and b will be changed to β and will be considered to be a function of τ. Then, in terms of a conductivity ratio,

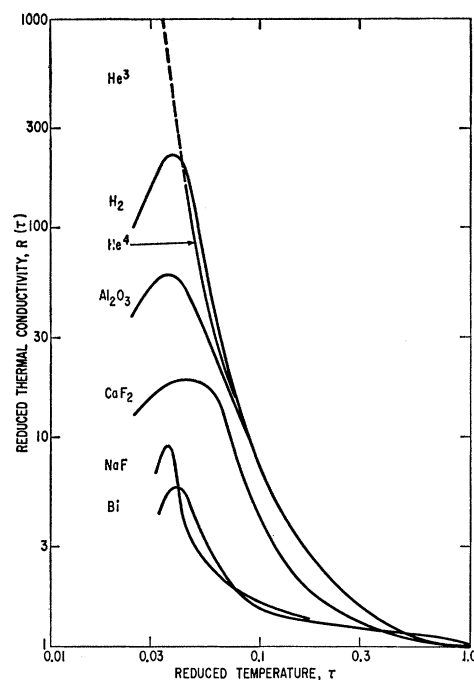$$K(T)/K(\theta) = f(\tau) = A' \exp(\beta^{-1}\tau^{-1})$$

FIG. 8. The reduced thermal conductivity $R(\tau)$ as a function of the reduced temperature, $\tau = T/\theta$. Included in this graph are a number of isotopically pure solids as well as CaF_2.

The requirement that $f(1)=1$, makes $A' = \exp(-1/\beta)$. Thus

$$f(\tau) = \exp[(1-\tau)/\beta\tau]. \qquad (10)$$

Furthermore if it is required that $K(T)$ vary as T^{-1} at $\tau = 1$, as is usually observed experimentally, then $\beta = 1$ at $\tau = 1$. At lower temperatures β will be greater than unity. The variation of β with temperature was computed from the composite curve for He^3, He^4, H_2, and Al_2O_3 in Fig. 8 using the relationship

$$\beta(\tau) = \frac{1-\tau}{\tau \ln(R/\tau)}. \qquad (11)$$

This curve is referred to in Fig. 9 as the exponential curve. For comparison, a curve of β vs τ was computed for the case where $K(T) = \tau K(\theta)$ at all temperatures, i.e. $R = 1$. This is the τ^{-1} curve in Fig. 9. The two curves are identical for $\tau \geq 1$, but, rapidly diverge at lower temperatures. For the exponential curve β has a asymptotic value of nearly 3. Often $K(T)$ curves are analyzed in terms of a "temperature-independent" exponential factor, b, as in Eq. (12). The value of b is defined as

$$b = -\frac{1}{\tau} \frac{d \ln\tau}{d \ln K}, \qquad (12)$$

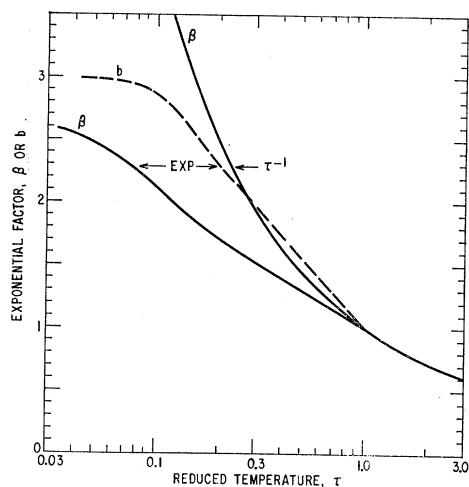over some limited range of temperature. The relation-

FIG. 9. The exponential factors, β and b, of a "universal" thermal conductivity curve $f(\tau)$ when only umklapp scattering is present. The reduced temperature is $\tau = T/\theta$. Also shown is a curve of β for the case where the "universal" function $f(\tau) = \tau^{-1}$.

ship between b and β is given by

$$b = \frac{\beta}{1 + (1-\tau)d \ln\beta/d \ln\tau}. \qquad (13)$$

This means $b \geq \beta$ at all temperatures $\tau \leq 1$. At $\tau = 1$, $b = \beta = 1$. From Fig. 9, b is nearly temperature independent for $\tau < 0.1$, and lies between 2.8 and 3.0. This compares with quoted[77] b values of 2.7 for diamond, 2.3 for He[4], and 2.1 for Al$_2$O$_3$.

The graph of β vs τ in Fig. 9 may be used to construct a curve of $K(T)$ vs T for any solid provided $K(\theta)$ and θ are known. Such a curve would probably serve as an upper limit to the thermal conductivity when umklapp processes are the dominant scattering mechanism. Such a curve has been constructed for CaF$_2$. This is shown as the dashed umklapp curve in Fig. 10, and lies somewhat above the measured curve.

At temperatures below 30°K in CaF$_2$, a combination of boundary and point impurity scattering determines the phonon thermal conductivity. If the crystal were chemically pure the only point impurities would be the Ca isotopes. These isotopes in combination with the boundary scattering determine the "boundary+isotopes" curve in Fig. 10. In order to construct this curve, the boundary plus isotope conductivity was first determined neglecting the effect of normal phonon processes using the method of Slack and Glassbrenner.[78] Then the normal phonon processes were introduced using the results of Ziman's variational method.[24] Ziman's method gives a thermal conductivity in the region above 20°K, where boundary effects can be

---

neglected, of

$$K(T) = 0.055 k^{\frac{5}{3}} \theta^3 m^{\frac{1}{2}} h^{-2} \gamma^{-1} (\Gamma^{-\frac{1}{2}} T^{-\frac{3}{2}}), \qquad (14)$$

where $k =$ Boltzmann's constant, $m =$ average mass of a single atom, $h =$ Planck's constant, and $\gamma =$ Grüneisen's constant. For isotope scattering Γ is given by Eq. (3). For chemical point impurity scattering Γ is[23]

$$\Gamma = \frac{1}{3}\sum_j V_0 \epsilon_{pj} S_j^2, \qquad (15)$$

where $V_0/3$ is the average volume occupied by one atom of the solid, ϵ_{pj} is the number of point impurities of type j per unit volume (see Table II), and S_j^2 is the total scattering number for the jth type of point imperfection. From Table II, some estimate of Γ(total) can be made.

$$\Gamma(\text{total}) = \Gamma(\text{isotope}) + \Gamma(\text{impurity}). \qquad (16)$$

For those elements present which have the same valence as Ca, i.e., Be and Sr, Γ is calculated from the mass difference. For the others, it is assumed that $S_j^2 = 1$. Values in the neighborhood of unity for S_j^2 have been suggested by the theory,[79] and have been found experimentally.[23] This procedure gives Γ(impurity) $= 20 \times 10^{-5}$, which is 30 times larger than Γ(isotope). At 30°K, the thermal conductivity as limited by isotopes would be 27 watts/cm deg from Eq. (14). The combination of impurities plus isotopes predicts a K value of 5 watts/cm deg. The observed value of 15 watts/cm deg from Fig. 10 is somewhere between these two calculated values. Such agreement is satisfactory,
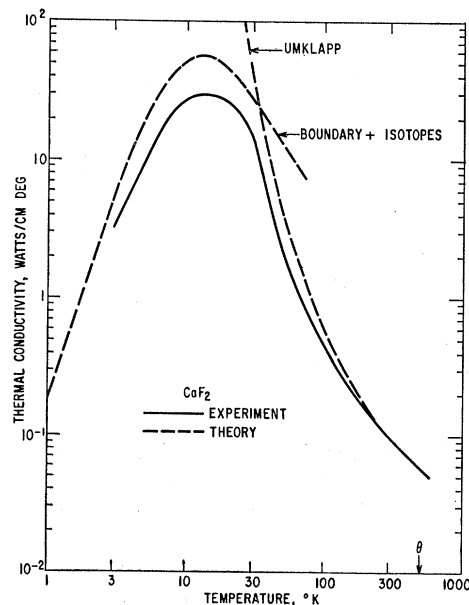

FIG. 10. Comparison of experiment and theory for the thermal conductivity of CaF$_2$. The dashed curves represent the upper limits to the thermal conductivity of chemically pure CaF$_2$ imposed by boundary, isotope, and umklapp scattering.

[77] R. Berman, F. E. Simon, and J. Wilks, Nature 168, 277 (1951).
[78] G. A. Slack and C. Glassbrenner, Phys. Rev. 120, 782 (1960).
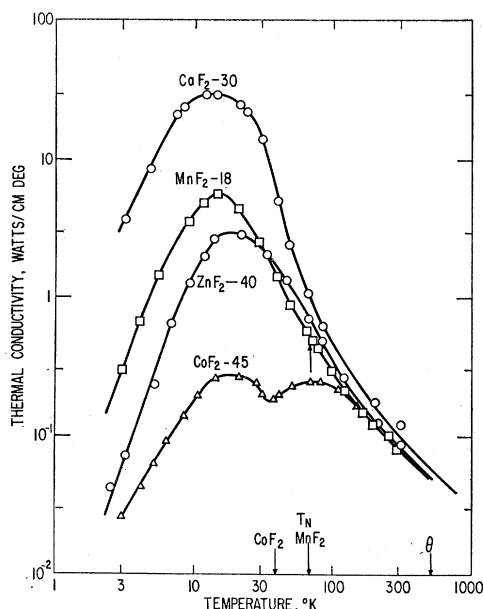[79] P. G. Klemens, Proc. Phys. Soc. (London) A68, 1113 (1955).

FIG. 11. The thermal conductivity of CaF_2, MnF_2, CoF_2, and ZnF_2 as a function of temperature. Above 30°K, the conductivity of the antiferromagnetic crystals is less than that of the diamagnetic ones.

and indicates that the crude approximations are good to within an order of magnitude. From these results, it is predicted that the CaF_2 crystal of the highest possible chemical purity, 1 cm in diameter, which contains the natural isotopes will not have a maximum thermal conductivity K_{max} greater than about 60 watt/cm deg at 15°K. The present crystal has a K_{max} only 50% of this. In order to approach 60 watt/cm deg, the total impurity concentration in the CaF_2 should be less than $10^{17}/cm^3$.

The results for ZnF_2, the other diamagnetic crystal, are similar to those of the CaF_2. The main exception is that the ZnF_2 is considerably less pure than the CaF_2. In the temperature range above 50°K, the thermal conductivities for ZnF_2 and CaF_2 in Fig. 11 are nearly the same. This is to be expected from the similarity of the K_θ' values in Table I. Below 50°K, the effect of point impurities drastically reduces the K of the ZnF_2. At 2°K, the measured K is only 4% of the K that would be imposed by the boundary limit. A crude estimate from the impurities listed in Table II gives Γ(impurity) $=100\times10^{-5}$, while Γ(isotope)$=1.98\times10^{-5}$. This large Γ is not sufficiently large to explain the very low thermal conductivity at low temperatures based on any simple point impurity scattering. The impurities may be particularly effective phonon scatterers at low temperatures by virtue of their strain fields as suggested by Carruthers[80] and by Pohl,[25] or by virtue of the magnetic moments in the dominant Fe and Ni impurities as suggested by experiments on paramagnetic and

ferrimagnetic crystals,[5,81-83] or by electronic excitation within the impurity centers.[84,85] Thus, it does not seem advisable to carry the analysis of the present results on ZnF_2 any further. The main point is that, except for impurity effects, the thermal conductivities of CaF_2 and ZnF_2 are very nearly equal. These two crystals span the transition metal fluorides that were measured, and thus serve as a comparison standard in which there is no phonon-magnetic moment scattering.

Paramagnetic Crystals

The MnF_2 and CoF_2 are paramagnetic above their respective Néel temperatures T_N of 67°K and 38°K. Above T_N, the magnetic moments are disordered, or at most exhibit only a residual short range order. As the temperature is reduced below T_N, the magnetic moments become progressively better ordered, until at 0°K there is a nearly complete long range order. A simple qualitative picture of the effect of this ordering process on the phonon-magnetic moment scattering can be given. Let us assume the following model in order to see how it agrees with the results.

In the paramagnetic state, all of the phonons are assumed to be scattered by the disordered magnetic lattice, and the scattering cross-section is independent of phonon wavelength. Thus, in this region above T_N, the phonon mean free path will be a combination of umklapp scattering and magnetic moment scattering. As the crystal is cooled to T_N and below, the magnetic lattice rapidly, but not instantaneously, becomes ordered. It is then assumed that the phonons are not scattered by the ordered magnetic lattice, but only by that fraction of it which is still disordered. This means that the phonon thermal conductivity increases rapidly below T_N until it becomes limited by umklapp, point impurity, or boundary scattering again.

Since any disturbance propagated in a periodic structure can conceivably transport energy, there must be some energy transport by magnons.[86-88] A magnon is just a propagated wave in the ordered lattice of the magnetic moments of the crystal. Then the total thermal conductivity is the sum of a phonon term K_g and a magnon term K_m,

$$K_{tot}=K_g+K_m. \qquad (17)$$

As discussed previously in the section on comparison of crystals, there is an appreciable magnetic heat capacity C_m, and there is also a propagation velocity v_m of magnons in these antiferromagnets. This velocity is

[80] P. Carruthers, Bull. Am. Phys. Soc. 5, 48 (1959).

[81] S. A. Friedberg and D. Douthett, Physica 24, S176 (1958).
[82] R. Berman, private communication.
[83] H. Rosenberg, Phil. Mag. 5, 1299 (1960).
[84] R. W. Keyes (Phys. Rev., to be published).
[85] J. Ziman, private communication.
[86] H. Fröhlich and W. Heitler, Proc. Roy. Soc. (London) A155, 640 (1936).
[87] I. Pomeranchuk, J. Phys. (U.S.S.R.) 4, 357 (1941).
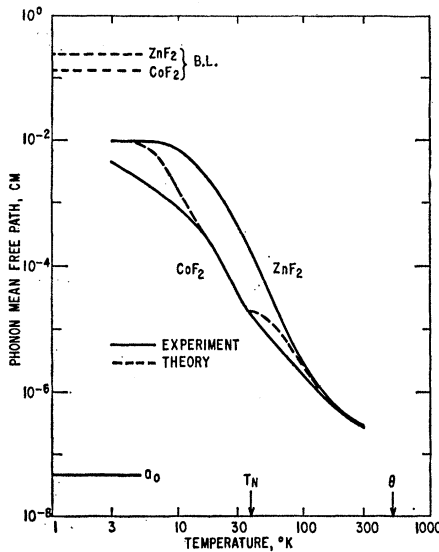[88] A. Akhieser and I. Pomeranchuk, J. Phys. (U.S.S.R.) 8, 216 (1944).

FIG. 12. The phonon mean free path for CoF_2 and ZnF_2 as a function of temperature. The lower dashed curve shows the application of a simple theory of phonon-magnon scattering to the CoF_2 results. The dashed curves labelled B.L. are the boundary limits imposed on the mean free path by the finite sample diameter. The lattice constant is a_0.

comparable to the phonon velocity. Hence K_m, given by

$$K_m = \tfrac{1}{3} l_m v_m C_m, \qquad (18)$$

might well be comparable to K_g if the mean free path of the magnons l_m is sufficiently large. From the experimental results in Fig. 11, it appears that K_{tot} of the magnetic fluorides is less than the K of the nonmagnetic ones above 30°K. Below 30°K, the situation is unclear because of the large content of chemical impurities. Thus, in the present experiments, it appears that $K_m \ll K_g$. This means l_m is quite small, perhaps as a consequence of strong magnon-magnon scattering. Therefore K_{tot} is very nearly equal to K_g. Throughout the present analysis this assumption is made.

The K_g term is given approximately by

$$K_g = \tfrac{1}{3} l_g \bar{v}_g C_g, \qquad (19)$$

where l_g is the phonon mean free path determined by a combination of scattering mechanisms, and C_g is the lattice specific heat capacity. The Debye approximation can be used to calculate C_g versus T from the θ values in Table I. Combining this with $\bar{v}_g$ from Table I and the measured K_g curves in Fig. 11, it is possible to compute $l_g(T)$ from Eq. (19). This has been done for ZnF_2 and CoF_2 in Fig. 12. It can be seen that for both crystals l_g is a monotonic function of temperature. Above the inflection point at 35°K, the l_g curve for CoF_2 is a combination of phonon-magnon scattering with a mean free path l_{gm} and umklapp scattering with l_{gu}. The value of l_g is determined by adding reciprocal mean free paths,[11]

$$l_g^{-1} = l_{gm}^{-1} + l_{gu}^{-1}. \qquad (20)$$

For l_{gu} of CoF_2, we can take the results for ZnF_2 as an approximation. Above the T_N of CoF_2, the value of l_{gm} is assumed to be temperature independent, and equal to $l_{gm}{}^0$. Below T_N, the fraction of disordered magnetic moments varies as $1 - (M/M_0)$, where M is $M(T)$, the magnetization of one cobalt sublattice[89] at temperature T, and M_0 is $M(0)$. Since l_{gm} is taken to be inversely proportional to the fraction of disordered spins, it is assumed that

$$l_{gm} = l_{gm}{}^0 [1 - (M/M_0)]^{-1}. \qquad (21)$$

For CoF_2, the $M(T)$ curve was computed using the Brillouin function $B_{\frac{3}{2}}(y)$ for a spin only moment of $S = \frac{3}{2}$, as found by Erickson[90] from neutron scattering measurements.

The dotted curve in Fig. 12 shows the computed results for CoF_2 using this simple model for l_{gm} and an $l_{gm}{}^0$ value of 2200 A. The agreement with the solid line, which is the experimental curve, is fair. Below 15°K, the higher impurity content of the CoF_2 compared to the ZnF_2 probably makes the experimental curve fall below the computed one. For temperatures above 35°K, the assumption of a constant value of l_{gm} equal to $l_{gm}{}^0$ may be incorrect, and a small temperature variation should be included. However, the qualitative behavior of this simple model agrees with the experiment, and it does not seem worthwhile to improve the model until measurements on better crystals are available. In Fig. 7, the minimum in the $K(T)$ curve for CoF_2 was found to lie at 35°K instead of 38°K which has been taken for T_N from specific heat measurements.[3] This difference is believed to be real, and represents differences in the way the magnetic disorder affects the two quantities.

The thermal conductivity results on MnF_2 in Figs. 6 and 11 do not show a pronounced dip in the curve at the T_N of 67°K. They do show a small change in slope, as mentioned previously, from $d \ln K_a(T)/d \ln T$ equals -1.8 to -1.6 as the temperature increases through T_N. This indicates the presence of some small amount of phonon-magnon scattering. By comparing the results on MnF_2 with those for ZnF_2 at 68°K, a value of $l_{gm}{}^0 = 4000$ A is estimated for MnF_2. This is about twice as large as the $l_{gm}{}^0$ of 2200 A for CoF_2. This difference between CoF_2 and MnF_2 may be associated with a larger orbital contribution to the magnetic moment in CoF_2 than in MnF_2 in the paramagnetic state. Such a suggestion has been made to account for differences in the piezomagnetic effects,[91] with which the phonon-magnon scattering should be closely associated.

The value of l_{gu} is 700 A at 67°K in MnF_2, whereas it is 20 000 A at 35°K in CoF_2. This rapid decrease in l_{gu} as T_N increases tends to greatly mask the phonon-

[89] T. Nagamiya, K. Yosida, and R. Kubo, Advances in Physics, edited by N. F. Mott (Taylor and Francis, Ltd., London, 1955), Vol. 4, p. 1.

[90] R. A. Erickson, Phys. Rev. 90, 779 (1953).

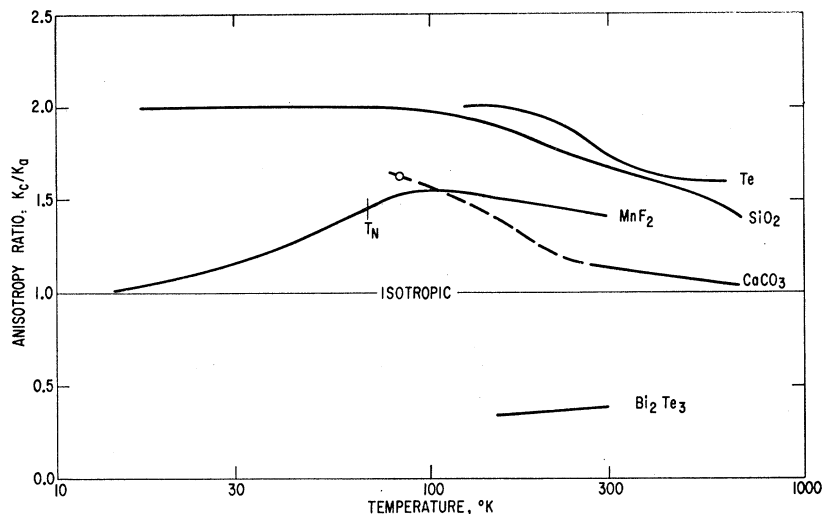[91] T. Moriya, J. Phys. Chem. Solids 11, 73 (1959).

FIG. 13. A composite curve of the anisotropy in the thermal conductivity of several crystals as a function of temperature. The anisotropy of MnF_2 disappears at at low temperatures, whereas that of SiO_2 does not.

magnon scattering in MnF_2 in comparison with CoF_2. For this reason, it is expected that measurements of the thermal conductivity of NiF_2 ($T_N = 73°K$) and FeF_2 ($T_N = 78°K$) would show practically no anomaly, whereas measurements on the corresponding chloride salts such as $CoCl_2$ ($T_N = 25°K$) might show substantial anomalies.

Anisotropic Thermal Conductivity

The temperature dependence of the anisotropy in K of the MnF_2 is interesting. Except in the boundary scattering region, where the sample size determines the thermal conductivity, the ratio $K_c/K_a \geq 1$. This ratio is equal to 1.42 at 300°K, reaches a maximum of 1.55 at 100°K, and approaches 1 below 15°K. Such anisotropy ratios have been studied for a number of materials[92,93] at room temperature, but only for a few single crystals such as $CaCO_3$,[74,94] SiO_2,[55,94–96] Te,[97] and Bi_2Te_3[98] have they been studied as a function of temperature. These four materials possess two principal thermal conductivities. One, K_c, along the c axis and two equal ones, K_a, perpendicular to the c axis. The anisotropy ratio for these four as well as for MnF_2 is shown in Fig. 13. The anisotropy in MnF_2 reaches its maximum at a temperature somewhat above the T_N of 67°K. There is no maximum in SiO_2, but rather a nearly constant value of $K_c/K_a = 2.0$ at temperatures below 70°K. Whether MnF_2 or SiO_2 is more nearly representative of the behavior of insulating solids is difficult to say. No very satisfactory theory of the anisotropy of thermal con-

ductivity exists, though various authors[99,100] have made some useful suggestions. From Fig. 13, it might be supposed that the magnetic contractions in MnF_2 below T_N tend to make the crystal more nearly cubic. However the measured contractions[4] below T_N tend to raise the $a_0/(c_0\sqrt{2})$ ratio from its 300°K value of 1.041. Thus, this is not the explanation of the asymptotic value of 1 for K_c/K_a at low temperatures. Further experiments on other anisotropic crystals are needed to solve this problem.

CONCLUSIONS

Crystals of the four divalent fluorides CaF_2, MnF_2, CoF_2, and ZnF_2 have nearly the same thermal conductivity at room temperature. The diamagnetic CaF_2 and ZnF_2 have thermal conductivities which can, for the most part, be explained by existing theories of phonon transport of the thermal energy limited by phonon scattering from phonons, isotopes, chemical impurities, and crystal boundaries. In the antiferromagnetic MnF_2 and CoF_2, the presence of phonon-magnon scattering reduces the thermal conductivity below that of the diamagnetic crystals. This reduction is particularly noticeable at the Néel temperatures of MnF_2 (67°K) and CoF_2 (38°K) where the phonon mean free paths for phonon-magnon scattering are 4000 A and 2200 A, respectively.

The thermal conductivity of MnF_2 is anisotropic at room temperature with $K_c/K_a = 1.42$. This anisotropy reaches a maximum at 100°K of 1.55 and decreases to 1.0 at 15°K.

The thermoelectric behavior of gold-cobalt thermocouples has been studied from 3°K–300°K. The absolute thermoelectric power of this alloy has been studied as a function of cobalt concentration, and an alloy of Au with 6%–8% Co is suggested as useful for thermo-

[92] K. Schulz, Fortschr. Mineral. Krist. Petrog. **9**, 221 (1924).
[93] M. S. Van Dusen, *International Critical Tables* (McGraw-Hill Book Company, New York, 1929), Vol. 5, p. 216.
[94] F. Birch and H. Clark, Am. J. Sci. **238**, 613 (1940).
[95] G. W. C. Kaye and F. W. Higgins, Proc. Roy. Soc. (London) **A113**, 335 (1926).
[96] W. J. de Haas and T. Biermasz, Physica **2**, 674 (1935); **4**, 752 (1937).
[97] K. I. Amirkanov, G. B. Bagduev, and M. A. Kazhlaev, Doklady Akad. Nauk S.S.S.R. **124**, 554 (1959).
[98] H. J. Goldsmid, Proc. Phys. Soc. (London) **B69**, 203 (1956).

[99] W. A. Wooster, Z. Krist. **95**, 138 (1936).
[100] E. Snitzer and C. R. Mingins, J. Chem. Phys. **29**, 1187 (1958).

couples. Such an alloy might be more stable and reproducible than the present 2% Co alloy.

Ultraviolet Absorption of the Mixed System KCl-KBr†

HERBERT MAHR

Laboratory of Atomic and Solid-State Physics, Cornell University, Ithaca, New York

(Received January 27, 1961)

The ultraviolet absorption of thin evaporated layers and the edge absorption of single crystals of the mixed system KCl-KBr were measured at room temperature in the photon energy range from 6–11 ev. In the thin layers, both the Cl⁻ and the Br⁻ absorption bands are present in the mixtures and their heights depend on the relative concentrations of the two ions. The energy values of the bands generally shift with composition, although in contrast to all the other bands, the high-energy KBr band shifts very little. The results obtained for the low-energy absorption bands can be described by a simple semiclassical electron transfer model. The behavior of the high-energy KBr band is discussed.

INTRODUCTION

PURE alkali halides are transparent throughout the visible into the ultraviolet range of the spectrum. There the absorption constant rises steeply to values above 10^5 cm^{-1}. As early as 1929, Hilsch and Pohl[1] found a series of rather sharp absorption maxima in this fundamental absorption region. They associated the first absorption band at the long-wavelength side with an electron transition from the halogen to the alkali ion. For the position of the absorption maximum, they gave the empirical formula

$$h\nu_{\max} = \alpha(e^2/r) + E - I, \qquad (1)$$

which fits the measurements within a few percent. Here $\alpha = 1.75$ is the Madelung constant for the NaCl structure, r the anion-cation distance, E the electron affinity of the halogen atom, and I the ionization energy of the alkali atom. Since then many investigators have extended the early measurements to higher photon energies and different temperature ranges. A recent comprehensive study by Eby, Dutton, and Teegarden[2] covered the absorption spectra of all alkali halides out to photon energies of more than 11 ev. Reflectivity measurements with single crystals by Hartman and co-workers[3] confirmed the results of the absorption measurements on thin evaporated layers.

Theoretical considerations concentrated on the first absorption maximum on the long-wavelength side, which was termed the exciton band.[4] Two models were proposed for the localized exciton in these ionic crystals. In one model the electron is transferred from the halogen ion to the nearest-neighbor alkali ions (electron-transfer model). The other model describes the exciton as an excited state of the halogen ion (excitation model). Attempts have also been made to classify the higher-energy absorption bands found experimentally in all alkali halides.[5]

Since it is difficult to correlate the various absorption bands in the different alkali halides, we have attempted to study the behavior of some particular bands under gradually varying conditions. For this reason, a system of mixed crystals of two alkali halides was used with the hope that it would provide more information about the nature of these absorption bands. Pick and Miessner[6] and Gnaedinger[7] used mixed crystals in a study of the F band and some V bands in the systems KCl-KBr and KCl-RbCl. Little information was obtained, however, on the influence of mixing in the fundamental absorption of the alkali halides. Hilsch and Pohl[1] measured an absorption maximum due to a 1% admixture of iodides to chlorides. For the case of the system KI-CsI

† Work supported by the Office of Naval Research and the Advanced Research Projects Agency.

[1] R. Hilsch and R. W. Pohl, Z. Physik **57**, 145 (1929); **59**, 812 (1930).

[2] J. E. Eby, D. Dutton, and K. J. Teegarden, Phys. Rev. **116**, 1099 (1959).

[3] P. L. Hartman, J. R. Nelson, and J. G. Siegfried, Phys. Rev. **105**, 123 (1957).

[4] For a survey, see the review articles by: H. Haken, Fortschr. Physik **6**, 271 (1958) and T. Muto, Progr. Theoret. Phys. (Kyoto) Suppl. No. **11**, 1 (1959).

[5] R. S. Knox and N. Inchauspé, Phys. Rev. **116**, 1093 (1959).

[6] H. Pick and G. Miessner, Z. Physik **134**, 576, 607 (1953).

[7] R. J. Gnaedinger, J. Chem. Phys. **21**, 323 (1953).